2024 IEEE International Conference on Robotics and Automation (ICRA 2024)
May 13-17, 2024. Yokohama, Japan

Energy Consumption Modelling of Coaxial-Rotor in Vortex Ring State for Controllable High-speed Descending

Jiawei Sun[1], Xiang Zhou[12], Taoze Ban[2], Jiannan Zhao[1*], Feng Shuang[1*].

***Abstract*— The ability to fast climb and descend is crucial for Unmanned Aerial Vehicle (UAV) applications in the mountains. The slower descent speed will affect the UAV's working efficiency in reaching the rescue area. However, during the fast descent of the rotorcraft, a chaotic flow field rampages as the rotorcraft falls into its wake flow. This is known as the vortex ring. Therefore, the safe descent velocity of consumer UAVs is usually limited to approximately 3m/s. This limitation reduces the potential of UAVs to execute tasks in mountainous and plateau regions. To broaden the task capability constrained by the maximum descending speed, it is necessary to jointly analyze the flow field and the energy consumption during descending. Existing research mainly focused on how to avoid entering the vortex ring instead of offering sufficient power to fly with it. In this paper, in order to achieve an efficient rotorcraft for rescuing in mountainous and plateaus, we break through the maximum-descending-speed of a coaxial rotors UAV. Hence, a power consumption managing pipeline is proposed to extend the power tolerance of the UAV. Specifically, a theoretic model for the coaxial rotors is proposed to analyze the induced velocity and energy consumption during vertical descending. Then, the theoretic model is verified to be consistent with the Computational Fluid Dynamics (CFD) and wind tunnel experiment results. Finally, we optimized the tolerance of the power and dynamic system according to the theoretic model. With this pipeline, our real-time flight achieved 8m/s controlled vertical-descent-speed (CVDS), which is a leading result in both quadrotors and coaxial UAVs.**

I. INTRODUCTION

In UAV tasks in the mountains, due to the efficiency of the rescue and limited battery load, it is necessary to descend faster. Current UAV products, such as Feimi's X8mini, have a maximum vertical descending speed (VDS) of 2m/s, and DJI's MAVIC3 drones limit the maximum VDS to 3m/s. While these speeds may meet the needs of the city environment, they are still incompetent for special task requirements such as rescuing in the mountains. The limitation of descending speed is a result of the complex airflow by rotors' wake, which can cause the UAV to lose stability and control, known as the vortex ring state (VRS). VRS, as shown in Fig. 1, is the leading issue in rotorcraft uncontrollable and excessive energy loss because the airflow constantly circles the propeller while hardly offering thrust [1], [2], [3].

This research was funded by the National Natural Science Foundation of China, grant number 62206065, and the Bagui Scholar Program of Guangxi.

[1] Guangxi Key Laboratory of Intelligent Control and Maintenance of Power Equipment, School of Electrical Engineering, Guangxi University, Nanning 530004, China.

[2]Co., Ltd. Mystical Bow Technology.

Fig. 1: The single rotor vortex ring state (VRS) during fast descending leads to instability, where the flow field is visualized by atomizer [4].

In Vertical Takeoff and Landing (VTOL) UAVs, the importance of efficient and safe landings has significantly increased due to their expanding range of applications [5], [6]. Since VRS is inevitable during high-speed descent, studying it to improve safety and task capability is necessary. Considering this, research during the first period focused on studying the critical factors to avoid VRS. In the 1970s, Wolkovitch discovered a qualitative judgment for a single rotor's vortex ring: when the induced velocity during decent is about 0.707 of that during hovering, the rotor is in the VRS [7]. Peters then pointed out that when the relative incoming flow velocity projection on the wake velocity direction becomes negative, the rotor is in the VRS [8]. This also means rotorcraft will meet the VRS as long as it descends faster. These prior studies on vortex rings built a significant basis for understanding the influence of the VRS.

These literature are not directly associated with extending the controlled vertical-descent-speed (CVDS). Considering the VRS flow, one skillful method to descend faster is adding an extra horizontal velocity to avoid the VRS using the yaw rate bang-bang control [9]. On the other hand, although the details of air movements in VRS are unpredictable, it is still possible to estimate global power consumption by analyzing the flow. With this hypothesis, we propose to extend CVDS by managing the energy consumption caused by VRS within the tolerance of the UAV. This paper demonstrates the following pipeline to extend the CVDS (see also Fig. 2):

- (1) Model the induced velocity on the plane of the rotor.
- (2) Build the relationship between power consumption and induced velocity.
- (3) Verify the theoretical model in experiments (CFD / wind tunnel experiment).
- (4) Extend the UAV's power tolerance and thrust tolerance according to the induced velocity model and the expected CVDS.

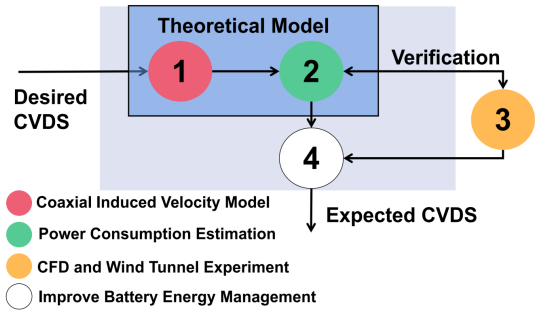

Fig. 2: Energy consumption management pipeline for extending CVDS.

Some literature provided the basis of our research: modeling of the single-rotor induced velocity, the description of VRS streamline, and CFD verification tools. For example, Wang proposed the truncated vortex tube model for flow-field analysis during rotorcraft descending [10]. Combing Wang's truncated vortex tube model, Perry established a model to calculate the induced velocity of the VRS [11]. Perry's model provides a theoretical basis for induced velocity modeling in CVDS. Some other research introduced the Biot-Savart law for modeling the induced velocity and verified their results in wind tunnel experiments [12], [13]. The usage of streamlines to describe airflow movement also inspires us to use streamlines for visually verifying the induced velocity model in extending CVDS [14] [15].

The above literature studied several methods for modeling the induced velocity in VRS but without power consumption analysis. Morden techniques like CFD can connect induced velocity theory and power consumption well. A few literature studies the CVDS of the coaxial UAV in VRS, e.g. Makeev combined CFD and wind tunnel experiment to study the coaxial rotors aerodynamic characteristics of the Kamov Ka-32 helicopter under high-speed descent [16] [17]. We also conducted CFD verification of our coaxial rotor and witnessed the vortex ring under 3-8 m/s descending speed, as shown in Fig. 3.

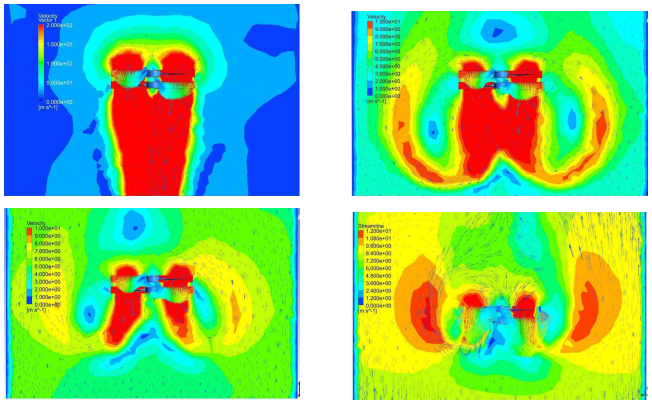

Fig. 3: 0, 3, 5, 8m/s Decent velocity flow field by CFD.

In summary, current research studied theoretical critical for VRS, velocity modeling, streamline for single rotors, CFD, and wind tunnel analysis for coaxial rotors [8] [10] [11]. But has neither studied the induced velocity model of coaxial UAV nor the power consumption management for extending CVDS. Therefore, The contribution of this paper is fourfold.

- Proposed the energy consumption managing pipeline for extending CVDS.
- The relationship between power consumption and flight states of the UAV during high-speed descending is revealed based on Bio-savart law, Wang and Perry's theory.
- Proposed the first model of induced velocity for coaxial rotors UAV in VRS.
- After carried a series of verification experiments, we improved the power and dynamic system for actual flight and achieved CVDS up to 8m/s.

The rest of this paper is organized as follows, Section II explains the process of calculating rotorcraft's power consumption in VRS. Section III presents the details of experiments. Specifically, the theoretic model is verified via CFD and wind tunnel experiments. With the confirmation of the theory, an optimized coaxial rotors UAV demonstrates the leading CVDS result (8m/s). Finally, we conclude this paper in Section IV.

II. Methodology

To ensure the power consumption for the coaxial rotors CVDS, this paper aims to reveal the relationship between the rotor power consumption (battery power required) and a given UAV vertical descent velocity. For the rotor power consumption accounts for approximately 80%-90% of the whole aircraft [18] reason, this paper mainly calculates the rotor-induced power for theoretic calculation.

In the following subsection, we will first formulate the problem of power consumption in theory. Next, the single rotor induced velocity model in literature is presented. After that, the single rotor model is extended to the case of the coaxial rotor. Finally, we use the above theoretic tools to calculate the power consumption of the coaxial UAV in VRS and cross-verify the results between CFD, and wind tunnel experiment.

A. Rotor Power Calculation

In CFD and experimental calculation, power consumption can be calculated by the rotor's rotation velocity and torque:

$$P = \omega\tau \tag{1}$$

Where the rotor torque τ can be acquired by CFD or torque sensor, the rotor speed ω can be acquired by CFD or the motor.

In theoretical calculation, the power consumption is calculated by thrust and the induced velocity

$$P_{theoretical} = Tv_i \tag{2}$$

Where v_i is the induced velocity in VRS, which can be deduced by the model of the rotor in VRS. T is the rotor thrust, also indicating the force acquired by the airflow. From

the basic theory of UAV's rotor [19], the thrust T can also be deduced by the induced velocity v_i:

$$T = 2\rho\pi R^2 v_i^2 \tag{3}$$

where ρ is the air density, R is the radius of the rotor.

Substitute Eq. (3) into Eq. (2), the theoretical power consumption of single rotor is:

$$P_{theoretical} = 2\rho\pi R^2 v_i^3 \tag{4}$$

Notably, Eq. (4) shows the induced velocity v_i is the significant variable for calculating the UAV power consumption.

According to the proposed pipeline, we will verify our theoretical model by comparing the streamline in CFD and streamline in theory. Next, we will build the single rotor descending model in VRS, and then the model is extended to coaxial case and verified its correctness.

B. Single Rotor Classic Descent Model

When analyzing the problem of vertical descent, the flow field around the rotor is regarded as a flow tube, and the velocity in the flow tube is uniformly distributed. First, without loss of generality, deduce the induced velocity of arbitrary point P in the flow tube, which is produced by a fluid element S making a cylindrical motion in space as shown in Fig. 4.

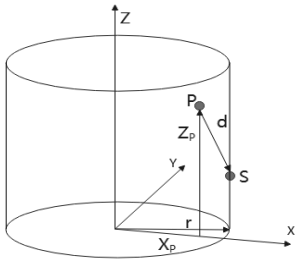

Fig. 4: Element S on the flow tube and arbitrary point P.

According to Wang [10], we use the tool of field description, the Biot-Savart law, to model the induced velocity. This theory describes that the induced velocity of an arbitrary point P in a flow field can be calculated via spatial density γ (Fig. 5).

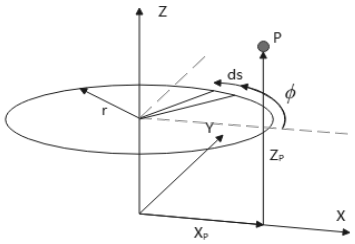

Fig. 5: Induced velocity model by Biot-Savart law [11].

According to Biot-Savart law, due to the rotation of the rotor, the resulting velocity at point P is calculated by:

$$dv(p) = \frac{\gamma dz}{4\pi d^3}\vec{ds}\times\vec{d} \tag{5}$$

where γ is the spatial density, dz is a distance element on Z axis, $\vec{ds}$ is an element vector on the rotor tip, $\vec{d}$ is the distance vector from s to point P.

The location of point P, vector $\vec{s}$ and $\vec{d}$ in circular cylindrical coordinate is given by:

$$\begin{aligned} p &= x_p i + z_p k \\ \vec{s} &= r\cos\phi\, i + r\sin\phi\, j + zk \\ \vec{d} &= (x_p - r\cos\phi)\, i - r\sin\phi\, j + (z_p - z)\, k \end{aligned} \tag{6}$$

Where ϕ is the angle between element s and the x-axis. Notably, the space density γ is affected by rotating speed Ω, rotor radius R, and descending velocity V_v.

$$\gamma = -\frac{N\Gamma_B\Omega}{2\pi V_v} = -\frac{C_T}{2}\frac{\overline{\Omega R}^2}{V_v} \tag{7}$$

Where, C_T is the lift coefficient, N is the number of blades, and Γ_B is the strength coefficient of vortex filaments. Combining the above equations (Eq.5- Eq.7), the radial velocity $-d\bar{v}_r(p)$, and axial velocity $-d\bar{v}_z(p)$ are given by:

$$-dv_r(p) = \frac{1}{2\pi V_v}\frac{f_\gamma(z)\left[\left(z_p - z\right)\cos\phi\right]d\phi dz}{\left[x_p^2 + 1 - 2x_p\cos\phi + \left(z_p - z\right)^2\right]^{3/2}} \tag{8}$$

$$-dv_z(p) = \frac{1}{2\pi V_v}\frac{f_\gamma(z)\left[1 - x_p\cos\phi\right]d\phi dz}{\left[x_p^2 + 1 - 2x_p\cos\phi + \left(z_p - z\right)^2\right]^{3/2}} \tag{9}$$

Where, $f_\gamma(z)$ is the strength of vorticity, which is equal to 1 when the vortex keeps along with the rotor plane, V_V is the descending velocity of the vortex along the tube edge, which is given by:

$$V_v = V_z + k(H)v_i \tag{10}$$

Where $k(H)$ is a variation of self-induced vorticity transport velocity with wake length, given by:

$$k(H) = 1 - 0.4e^{(-H/2)^2} \tag{11}$$

According to Wang, H is approximated to zero in VRS, leading to a constant $k(H) \approx 0.6$.

So far, Wang's theory can calculate the induced velocity in the descent of the UAV. However, Wang's model only calculates the average induced velocity in the direction along the tube, without considering the vortex at the rotor tip. Furthermore, we consider the induced velocity caused by VRS to contain the velocity on the rotor tip (tip vortex) and the velocity near the rotor (flow tube). Therefore, a mathematical model of the vortex at the rotor tip needs to be added.

As shown in Fig. 6, Perry [11] assumes a vortex with radius R_c at the tip of the rotor, and the velocity distribution is uniform between R_c and ηR_c. The induced velocity du is

generated by an element in the vortex at the rotor tip. We assume the vortex at the rotor tip consumes power mainly from its vertical component dW, given by:

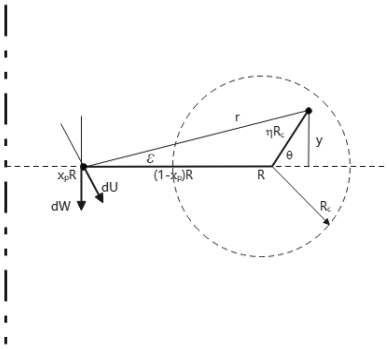

Fig. 6: Model of induced velocity based on a straight line vortex with a core of uniformly distributed vorticity [11].

$$
\begin{aligned}
dW &= \frac{d\gamma}{r}\cos\varepsilon \\
&= \frac{\gamma_0}{\pi\left(1-\eta_0^2\right)R}\frac{\frac{R_c}{R}\cos\theta\eta+\left(1-x_p\right)}{\frac{R_c^2}{R^2}\eta^2+2\left(1-x_p\right)\frac{R_c}{R}\cos\theta\eta+\left(1-x_p\right)^2} \\
&\quad\times\eta d\eta d\theta
\end{aligned}
\tag{12}
$$

Where r is The distance from the average distribution area to an arbitrary point x_p on the rotor, η is the proportion factor of R_c. Then we integral the dW:

$$
\begin{aligned}
W =& \frac{\gamma_0}{\pi\left(1-\eta_0^2\right)R}\frac{R_c}{R}\cdot \\
&\int_0^{2\pi}\int_0^1 \frac{\eta^2 d\eta}{\frac{R_c^2}{R^2}\eta^2+2\left(1-x_p\right)\frac{R_c}{R}\cos\theta\eta+\left(1-x_p\right)^2}\cos\theta d\theta \\
&+\frac{\gamma_0}{\pi\left(1-\eta_0^2\right)R}\left(1-x_p\right)\cdot \\
&\int_0^{2\pi}\int_0^1 \frac{\eta d\eta}{\frac{R_c^2}{R^2}\eta^2+2\left(1-x_p\right)\frac{R_c}{R}\cos\theta\eta+\left(1-x_p\right)^2}d\theta
\end{aligned}
\tag{13}
$$

We assume that the vortex at the rotor tip mainly influences the induced velocity at the rotor plane in the vertical direction. Therefore, the average radial induced velocity can be directly integrated by Eq. (8):

$$
\begin{aligned}
v_r(p) =& \frac{1}{2\pi V_v}\int_0^{2\pi}\frac{\cos\phi d\phi}{\sqrt{x_p^2+1-2x_p\cos\phi+\left(z_p-H\right)^2}}d\phi \\
&-\frac{1}{2\pi V_v}\int_0^{2\pi}\frac{\cos\phi d\phi}{\sqrt{x_p^2+1-2x_p\cos\phi+z_p^2}}d\phi
\end{aligned}
\tag{14}
$$

For rotor power consumption calculation, the whole induced velocity is the vector sum between radial and vertical induced velocity:

$$
\vec{V}_i = \vec{W}+\vec{V}_r \tag{15}
$$

Where W is the vertical component of induced velocity, $\vec{V}_r$ is the component in the radial direction. Then, the induced velocity for power consumption is calculated by:

$$
V_i = \sqrt{\left|\vec{W}\right|^2+\left|\vec{V}_r\right|^2} \tag{16}
$$

Up to now, we have given the induced velocity model of a single rotor and deduced the equation of induced velocity for power consumption. Next, this induced velocity model of VRS is extended to coaxial rotors case.

C. Coaxial-rotor Vortex Ring Model

Due to the aerodynamic interaction of the upper and lower rotor in coaxial UAV, the flow at the lower rotor was affected by the upper rotor's wake [19]. On the lower rotor, the airflow can be divided into two parts with different induced velocities, the part affected by the upper rotor's wake and the part that is not, as shown in Fig. 7.

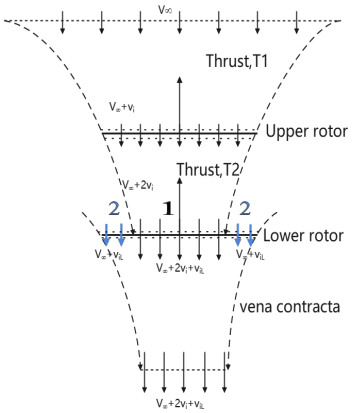

Fig. 7: Flow model assumed for coaxial propellers in an axial flow using momentum theory [19]. Numbers 1 and 2 denote the contraction rate of the upper rotor's wake.

Our CFD flow field analysis showed that there is no significant difference in vena contracta between hovering and VRS. Reasonably, we assume that the coaxial UAV in the VRS still maintains the aerodynamic interference and takes the empirical value of $0.78R$ as the wake contraction rate [20]. Considering this is a strong assumption, it is verified by numerical calculation and streamline morphology analysis [1].

The vector of the lower rotor's induced velocity is given by:

$$
\vec{V}_{ilow} = \vec{V}_{ilow1}+\vec{V}_{ilow2} \tag{17}
$$

Where $\vec{V}_{ilow1}$ is the part belonging to the vena contract, and $\vec{V}_{ilow2}$ is the part without interference from the upper rotor, they can be divided into the vertical part and the radial part:

[1]The numerical calculation comparison is presented in Table I, while the streamline analysis is shown in Fig. 8

$$\begin{cases} \vec{V}_{ilow1} = \vec{W}_1 + \vec{V}_{r1} \\ \vec{V}_{ilow2} = \vec{W}_2 + \vec{V}_{r2} \end{cases} \tag{18}$$

Thus, $\vec{V}_{ilow1}$ and $\vec{V}_{ilow2}$ can be deduced by substituting $0.78R$, and $0.22R$ into the single rotor's model (Eq. (13) and Eq. (14)) for the part affected by the upper rotor's wake and the part that is not.

According to the proposed pipeline, this theoretical induced velocity is verified by streamline analysis with comparison against CFD result (Fig. 8). The interference between the upper and lower rotor is similar, and the vortex near the rotor tip also exhibits a very similar shape. This similarity indicates that our assumption, which posits that the vena contracta is not significantly affected by the VRS, is reasonable.

Finally, the magnitude of induced velocity for power consumption calculation is given by:

$$V_{ilow} = \sqrt{(W_1 + W_2)^2 + (V_{r1} + V_{r2})^2} \tag{19}$$

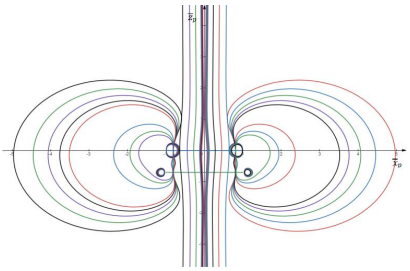

(a)

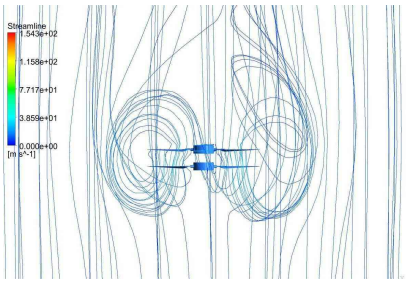

(b)

Fig. 8: Streamline comparison between the theoretical model and CFD simulation. (a) The streamline is plotted from vertical and radial induced velocities. (b) Streamline by CFD.

Thus, the power consumption of the whole coaxial rotors UAV can be calculated by:

$$P = 2\rho\pi R^2 (V_i + V_{ilow})^3 \tag{20}$$

D. Calculation of Realistic UAV Power Consumption

This paper assumes an expected descending speed of 8m/s, the body weight of $6.5kg$, a designed rotor speed of $3300rpm$, and a rotor diameter of $24inches$ (Tabel I). With these design parameters, the thrust and induced power can be estimated. Substitute $8m/s$, $3300rpm$, $24inch$, into Eq. (20). Also, the theoretical thrust can be calculated by Eq. (3),

TABLE I: UAV Design Parameters and Calculation Results

Parameter Names	Parameters	Calculation Items	Results
Expected Decent Velocity	8m/s	Theoretic Power Consumption	882.49W
Rotor Size	24inch	CFD Power Consumption	883.2W
Rotor Speed	3300rpm	Theoretic Thrust	79.28N
Hovering Thrust	70.84N		

and the result is $79.28N$. As we can see, the theoretically expected thrust ($79.28N$) is larger than the actual hovering thrust ($70.84N$). To control the UAV recovery from the VRS, the maximum thrust T_{max} of the dynamic system should be redundant (40% redundancy in this paper) for safety. According to this, we can calculate the redundant T_{max} is $110.9N$. Therefore, the instantaneous power of the battery should be more than $1286.3W$ according to Eq. (2).

For UAV power consumption in CVDS, with the above calculation, we choose a battery with $648Wh$ capacity and nominal power with $1296W$. Theoretically, the designed coaxial UAV can work for 0.5 hours in CVDS with the ability to recover. The designed parameters and calculated power consumption results are summarised in Table I [2]. The next section will verify the theoretical calculations using CFD and wind tunnel tests.

III. Coaxial UAV Experiment

In this section, the designed coaxial UAV is verified by CFD power estimation, wind tunnel experiment, and real-time flight demonstration. To verify the theoretical model, the CFD and wind tunnel experiments are compared at different descending velocities.

The power consumption result for comparison and verification is shown in Fig. 9. It can be seen that the error rate is less than 3.92%. This result supports our model for power consumption estimation for coaxial UAV's high-speed descending.

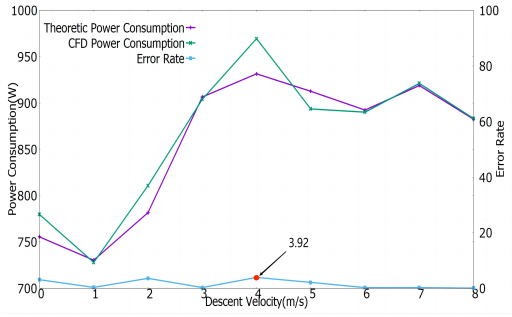

Fig. 9: Comparison between theoretical model and CFD estimated power consumption for different CVDS.

We further conducted a wind tunnel experiment based on the theoretical calculation and CFD analysis. The test bench uses the six-dimensional force sensor to measure lift and

[2]Please note the theoretic power consumption and theoretic thrust are the minimum value for the controllable (can be recovered) vertical descent at the expected descent velocity.

torque. During the experiment, the test bench will place in the wind tunnel's wind field, and the rotor is located in the center of the wind field (Fig. 10). The wind tunnel velocity is set to 0, 3, 5, and 8m/s, and the rotor speed is 3300rpm. The thrust is obtained in the upward direction along the fuselage axis. In wind tunnel experiments, the thrust data from the six-dimensional sensor is the most accurate data [3]. It further confirmed the correctness of our theoretical model. As shown in (Fig. 11), because the theory is not suitable for calculating the hover state, we ignore the error rate 6.9%, and the maximum error rate of the descending state is 3.47%. With this error rate, we consider that the theoretical results are almost consistent with reality.

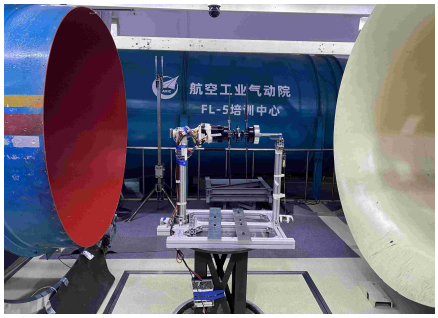

Fig. 10: Wind tunnel test scenario.

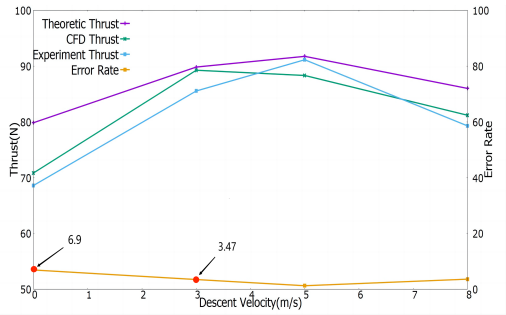

Fig. 11: Thrust comparison between theoretic, CFD estimated, and wind tunnel experiment results for different CVDS.

After verifying the CFD and wind tunnel test, according to the pipeline, we carried out the real-time flight. The records of real-time high-speed descending (Fig. 12) show that the descent rate has reached 8m/s, and the whole descending process is controllable with the ability to recover. This result reflected the effectiveness of the proposed pipeline and our redundant battery management design.

IV. CONCLUSIONS

This paper proposes a pipeline for extending the controlled vertical descending speed (CVDS) by managing power consumption to improve the time efficiency of UAV applications in mountainous and plateau regions. This pipeline is applied to coaxial rotors, expecting to break through the maximum descending speed of rescuing UAVs. Following the proposed pipeline, a theoretical model is built, and then, we compare CFD simulation and wind tunnel experiments to verify the theoretical model and UAV design. Finally, the real-time fast descending flight is conducted and achieved $8m/s$ CVDS, which is the leading result in both coaxial rotors and quadrotors. This high-speed descent meets our expectations, proving that UAVs can still work with VRS and are controllable, while, on the other hand, it could be used for high-speed descending. Based on the proposed safety power management in VRS, it is worth designing an auto-control law for faster and long-distance CVDS in the future.

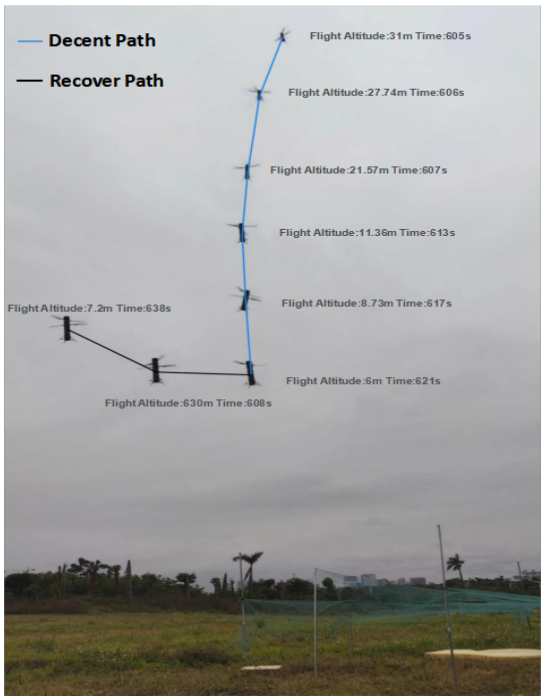

(a) Trajectory during fast descent.

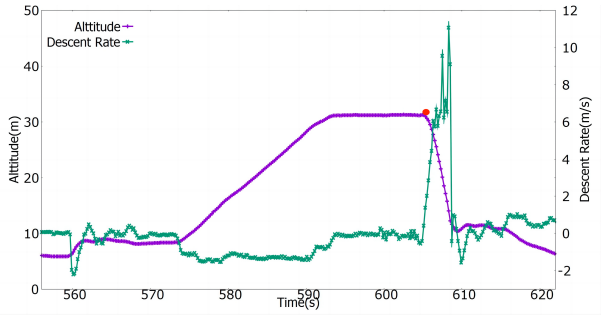

(b) Alttitude and descent rate records.

Fig. 12: CVDS verification by Coaxial UAV fast descent in actual flight. The red circle denotes the start point of the descending process.

[3]Overheating of motors during long-period experiments will affect its own efficiency, causing inaccuracy in direct power estimation via current and voltage.

REFERENCES

[1] SKYbrary, "Vortex ring," https://skybrary.aero/articles/vortex-ring, accessed2022.12.16.

[2] H. F. Handbook, "Faa-h-8083-21a," *United States Department of Transportation, Federal Aviation Administration, Airman Testing Branch*, 2019.

[3] Aerossurance, "Vortex ring state: Virginia state police bell 407 fatal accident," https://aerossurance.com/helicopters/vrs-virginia-state-police-b407/, accessed2022.12.16.

[4] V. H. Services, "Aerial footage of the vuichard vortex recovery in 5k quality," https://www.valair.ch/en/news-en/aerial-footage-of-the-vuichard-vortex-recovery-in-5k-quality/, accessed2017.10.10.

[5] N. Çabuk, "Design and experimental validation of an adaptive landing gear for safe landing on uneven grounds of vtol uavs in the context of lightweight and fast adaptations," *Arabian Journal for Science and Engineering*, pp. 1–14, 2023.

[6] J. Park, I. Kim, J. Suk, and S. Kim, "Trajectory optimization for takeoff and landing phase of uam considering energy and safety," *Aerospace Science and Technology*, vol. 140, p. 108489, 2023.

[7] J. Wolkovitch, "Analytical prediction of vortex-ring boundaries for helicopters in steep descents," *Journal of the American Helicopter Society*, vol. 17, no. 3, pp. 13–19, 1972.

[8] D. A. Peters and S.-Y. Chen, "Momentum theory, dynamic inflow, and the vortex-ring state," *Journal of the American Helicopter Society*, vol. 27, no. 3, pp. 18–24, 1982.

[9] A. Talaeizadeh, H. N. Pishkenari, and A. Alasty, "Quadcopter fast pure descent maneuver avoiding vortex ring state using yaw-rate control scheme," *IEEE Robotics and Automation Letters*, vol. 6, no. 2, pp. 927–934, 2021.

[10] W. Shi-cun, "Analytical approach to the induced flow of a helicopter rotor in vertical descent," *Journal of the American Helicopter Society*, vol. 35, no. 1, pp. 92–98, 1990.

[11] F. J. Perry, W. Y. Chan, I. A. Simons, R. E. Brown, G. A. Ahlin, B. M. Khelifa, and S. J. Newman, "Modeling the mean flow through a rotor in axial flight including vortex ring conditions," *Journal of the American Helicopter Society*, vol. 52, no. 3, pp. 224–238, 2007.

[12] W. Johnson, "Model for vortex ring state influence on rotorcraft flight dynamics," Tech. Rep., 2005.

[13] A. Karpatne, J. Sirohi, S. Mula, and C. Tinney, "Vortex ring model of tip vortex aperiodicity in a hovering helicopter rotor," *Journal of Fluids Engineering*, vol. 136, no. 7, 2014.

[14] J. Thomas, "Vortex filament dynamics," 2015.

[15] C.-J. Kim, S. H. Park, S. K. Sung, and S.-N. Jung, "Dynamic modeling and analysis of vortex filament motion using a novel curve-fitting method," *Chinese Journal of Aeronautics*, vol. 29, no. 1, pp. 53–65, 2016.

[16] P. Makeev, Y. Ignatkin, and A. Shomov, "Numerical study of coaxial main rotor aerodynamics in steep descent," *Aerospace*, vol. 9, no. 2, p. 61, 2022.

[17] P. V. MAKEEV, Y. M. Ignatkin, and A. I. SHOMOV, "Numerical investigation of full scale coaxial main rotor aerodynamics in hover and vertical descent," *Chinese Journal of Aeronautics*, vol. 34, no. 5, pp. 666–683, 2021.

[18] H. Van Vyve, P. Chatelain, and G. Winckelmans, "Simulation of a helicopter in vortex ring state through a coupled simulation of multi-body dynamics and aerodynamics."

[19] G. J. Leishman, *Principles of helicopter aerodynamics with CD extra*. Cambridge university press, 2006.

[20] U. Saetti, J. Enciu, and J. F. Horn, "Performance and design optimization of the f-helix evtol concept," in *Proceedings of the Vertical Flight Society's 75th Annual Forum and Technology Display, Philadelphia, PA, USA*, 2019, pp. 13–16.